IEEE Photonics Journal
An IEEE Photonics Society Publication

Open Access

Temperature-Insensitive Frequency Conversion by Electro-optic Effect Compensating for Phase Mismatch

Volume 8, Number 5, October 2016

Zijian Cui
Dean Liu
Aihua Yang
Jie Miao
Junyong Zhang
Jianqiang Zhu

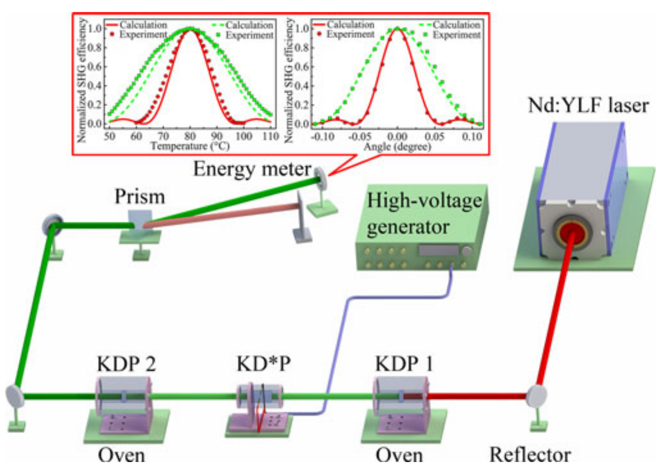

DOI: 10.1109/JPHOT.2016.2614912
1943-0655

Temperature-Insensitive Frequency Conversion by Electro-optic Effect Compensating for Phase Mismatch

Zijian Cui,[1,2] Dean Liu,[1] Aihua Yang,[1,2] Jie Miao,[1] Junyong Zhang,[1] and Jianqiang Zhu[1]

[1]Key Laboratory of High Power Laser and Physics, Shanghai Institute of Optics and Fine Mechanics, Chinese Academy of Sciences, Shanghai 201800, China
[2]University of Chinese Academy of Sciences, Beijing 100049, China

DOI:10.1109/JPHOT.2016.2614912
1943-0655

Manuscript received August 20, 2016; revised September 28, 2016; accepted September 29, 2016. Date of publication October 4, 2016; date of current version October 19, 2016. Corresponding author: D. Liu (e-mail: liudean@siom.ac.cn).

Abstract: A universal phase mismatch compensation method, which can be applied to temperature-insensitive frequency conversion, is experimentally demonstrated. In this method, two nonlinear crystals and an electro-optic crystal are cascaded. The generated phase mismatch in the nonlinear crystal can be well compensated for in the electro-optic crystal, thereby improving the stability of frequency conversion. In the proof-of-principle experiment, temperature-insensitive second and third harmonic generation (SHG and THG) are investigated by cascading KH_2PO_4 (KDP) and KD_2PO_4 (DKDP) crystals. The experimental results show that the temperature acceptance bandwidths of SHG and THG are 2.1 and 2.3 times larger, respectively, than that of the traditional method employing a single crystal. Meanwhile, the effectiveness of this method is also analyzed at a high power density, and a solution for the case of a nonuniform temperature is also discussed. Furthermore, angle-insensitive SHG is demonstrated to prove that this method can significantly reduce the influence of various unfavorable factors on frequency conversion. The demonstrated method may have potentially important applications in the nonlinear optical frequency conversion system.

Index Terms: Nonlinear optics, second and third harmonic generation (SHG and THG), cascaded nonlinear processes.

1. Introduction

Frequency conversion based on the second-order nonlinear optical effect is an important nonlinear optical process. With recent developments in laser science and technology, frequency conversion plays an increasingly important role in the fields of fundamental research and technological application [1]–[4]. In order to achieve high frequency conversion efficiency, satisfying phase matching (PM) is a basic condition [4]. However, in practical applications, slight changes in the nonlinear crystal (e.g., angle or temperature variation) can lead to a phase mismatch and will have an unfavorable effect on the frequency conversion [5]–[7]. In particular, in the large laser systems, there are high demands for the frequency conversion. For example, the National Ignition Facility (NIF), which is composed of 192 individual high-power laser beams, requires that the precision of the balance of output energy and power between the beams be $<3\%$ and $<8\%$ (beam to beam), respectively

[8]. These precision requirements were the basis for a series of laser investigations completed at the NIF [8], [9]. Therefore, the temperatures and angles of the crystals need to be controlled with high precision and stability. However, for the whole large laser systems, it is very difficult to achieve among multi-beams.

When the phase matching condition is not satisfied, a phase mismatch will occur ($\Delta k \neq 0$), and the phase mismatch value (PMV) of the interacting waves accumulates ($\Delta K = \Delta k \times l$) with the propagation distance (l) in the crystal. If the PMV is not compensated for during the frequency conversion process, the rate of conversion efficiency will gradually decrease as the PMV accumulates. Once the transmission distance reaches half the coherence length (coherence length is defined by $l_c = 2\pi/\Delta k$), PMV will be accumulated to π and back-conversion will occur. The conversion efficiency will reduce significantly and the output energy will become unstable. If PMV is compensated for before back-conversion occurs and makes it up to an integer multiple of 2π, the frequency conversion will continue effectively. In this situation, the conversion efficiency increases monotonically during the entire frequency conversion process and the stability of frequency conversion can, thus, be significantly improved.

In order to reduce the influence of unfavorable factors on frequency conversion, some methods, which are used to suppress or compensate for the phase mismatch, have been proposed to improve the conversion efficiency [10]–[15]. However, they are mainly applied to a single beam over a small range or are limited by many factors (e.g., crystal type, PM type or laser wavelength). What's more, these methods are aimed at the phase mismatch arising from a specific cause. Actually, there is more than one cause of the phase mismatch in practical applications.

At present, there are some reports on the realization of wavelength tunable optical parametric oscillation and modification of the spectral shape of the parametric-gain based on electro-optic effect [16], [17]. Recently, we theoretically analyzed a universal method that can compensate for the temperature induced phase mismatch by electro-optic effect [18]. In this paper, the proposed method is experimentally demonstrated and further studied. The feasibility and validity of this method is verified by temperature insensitive second and third harmonic generation (SHG and THG) at 1053 nm in KH_2PO_4 (KDP) crystals. Meanwhile, angle insensitive SHG is also experimentally achieved. The experimental results show that this method can significantly reduce the influence of various unfavorable factors on frequency conversion, which is unexpected based on the prior work. In addition, the effectiveness of this method is analyzed at a high power density, the lengths of crystals are further optimized to achieve a better effectiveness, and a solution for the case of a non-uniform temperature is given, which has not been solved in prior work.

The basic experiment scheme is that two nonlinear crystals are cascaded and an electro-optic crystal is placed between them. PMV will generate because of electro-optic effect when the waves pass through the electro-optic crystal, and it varies with the voltage [18]. Thus, the accumulated PMV in the first nonlinear crystal can be well compensated for in the electro-optic crystal by adjusting the voltage when the phase mismatch occurs. In the next nonlinear crystal, the frequency conversion can effectively continue. Because the voltage has excellent tunability and exhibits high-precision control, this method can rapidly and precisely compensate for the phase mismatch arising from different causes (e.g., crystal angle, temperature variation or beam tilt). Therefore, the influence of various unfavorable factors on frequency conversion can be reduced.

2. Experimental Details of Temperature Insensitive Frequency Conversion

In the proof-of-principle experiment, a Q-switched Nd:YLF laser at 1053 nm with a Gaussian pulse duration of 10 ns was used as the fundamental laser source. The transverse spatial profile is a circular flat-top with a diameter of 8 mm, a pulse repetition rate of 0.1 Hz, and the typical output pulse energy of 550 mJ. The peak power density is approximately 100 MW/cm^2. Two 12 mm $\times$ 12 mm $\times$ 6.25 mm and two 12 mm $\times$ 12 mm $\times$ 5.5 mm KDP crystals are cut for type-I (o + o $\rightarrow$ e) and type-II (e + o $\rightarrow$ e) PM ($\theta_I = 41.3^\circ$, $\varphi_I = 45^\circ$ and $\theta_{II} = 59.2^\circ$, $\varphi_{II} = 0^\circ$) to generate second and third harmonic (SH and TH), respectively. A 30 mm long KD_2PO_4 (KD*P) crystal (cutting angle $\theta = 90^\circ$, $\varphi = 45^\circ$) and a high-voltage pulse generator (Lasermetrics 5046ER, operating voltage range: 0–12 kV,

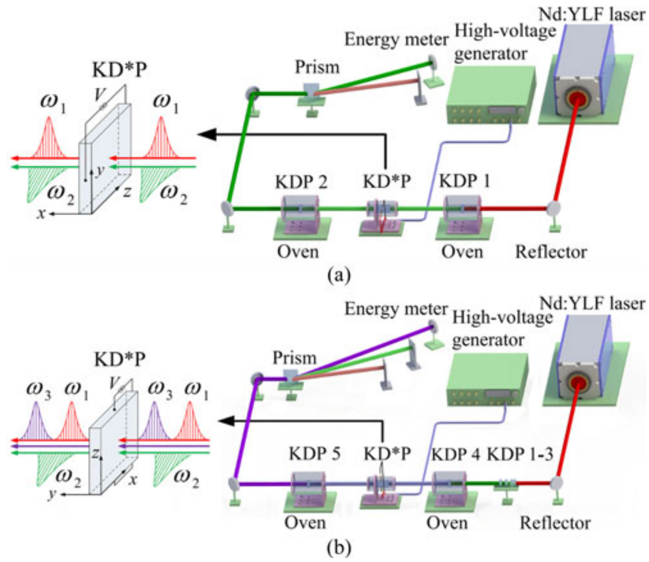

Fig. 1. Experimental setup for temperature insensitive (a) SHG and (b) THG.

voltage regulation precision: 0.2 kV) are employed to compensate for the phase mismatch. All the transparent surfaces of the crystals were polished and coated with three-wavelength antireflection film (Transmittance $>$ 99%) at 1053, 526.5, and 351 nm.

The experimental setups for temperature insensitive SHG and THG are shown in Fig. 1. Transverse electro-optic modulation is used, and the direction of the electric field is always along the z-axis of the KD*P crystal. The beams propagate along the x and y axes of the KD*P crystal for SHG [see Fig. 1(a)] and THG [see Fig. 1(b)], respectively, where ω_1, ω_2 and ω_3 represent the fundamental wave (FW), SH, and TH; x, y, and z are the new principal optic axes in the presence of an external electric field applied parallel to the z-axis of KD*P crystal.

In the SHG experiment, the KDP crystals for SHG are mounted in two ovens where the temperature can be varied from 40 to 180 °C with a precision of $\pm$0.1 °C. The temperature of the electro-optic crystal remains stable at room temperature. The SH is separated from the FW by a prism. In THG, the frequencies ω_i ($i = 1, 2, 3$) satisfy the relationship $\omega_3 = \omega_2 + \omega_1$. Matching the photon-number of the FW (ω_1) and the SH (ω_2) is an important constraint for THG efficiency. In order to obtain a high THG efficiency, the SHG efficiency cannot be too low. Since the power density of the FW is relatively low, three KDP crystals (one 12.5 mm long and two 6.25 mm long) for SHG are cascaded to improve the SHG efficiency. In order to analyze the influence of temperature on THG efficiency, two KDP crystals for THG are mounted in the oven. Both the KDP crystals for SHG and the KD*P crystal are at room temperature. The TH is separated from the FW and the SH by a prism.

We define the SHG and THG efficiencies by $\eta_2 = E(\omega_2)/E(\omega_1)$ and $\eta_3 = E(\omega_3)/E(\omega_1)$, respectively, where $E(\omega_1)$ is the initial energy of the FW, $E(\omega_2)$ is the energy of the SH emitted from KDP 2 [as shown in Fig. 1(a)], and $E(\omega_3)$ is the energy of the TH emitted from KDP 5 [as shown in Fig. 1(b)]. According to the calculated results for the temperature acceptance bandwidth (TAB) and the temperature control range of the ovens, the initial PM temperature was set to 80 °C. The type-I SHG and type-II THG at 1053 nm were studied within variable temperature ranges of 50–110 and 70–90 °C, respectively. Because the refractive indices of the crystals have a linear relationship with temperature [19], similar results can be obtained for the room temperature case. We varied the temperature of the nonlinear crystals over the stated ranges in increments of 1.0 °C. The output SHG and THG energies were measured 30 times at each temperature and the average values were considered, in order to eliminate the influence of energy fluctuation. In order to intuitively compare the temperature acceptance bandwidth of our demonstrated method with the traditional method, as

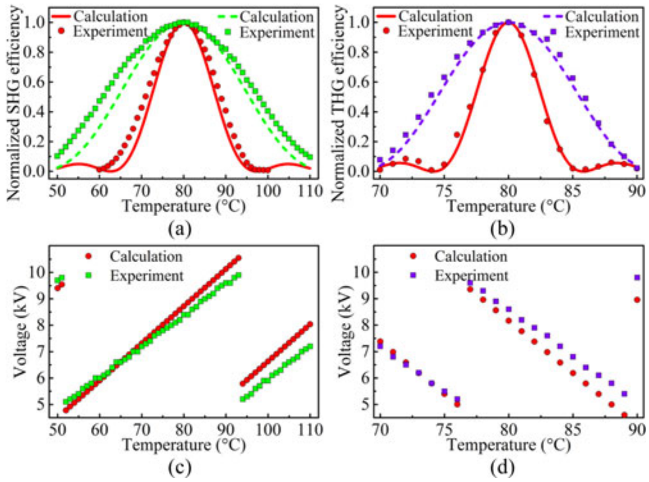

Fig. 2. Experimental and calculated (a) SHG and (b) THG efficiencies. (c) SHG and (d) THG phase mismatch compensation voltages versus temperature. In (a) and (b), the solid line and circle symbols indicate the traditional method; the dashed line and square symbols indicate our proposed method, and all efficiencies are normalized to their maximum values at the initial PM temperature.

well as that of the theoretical results with the experimental results, all efficiencies are normalized to their maximum values at the initial PM temperature. The experimental results are shown in Fig. 2.

Fig. 2(a) shows how SHG efficiency varies with temperature. The measured maximum SHG efficiency of 5.2% was measured when the KDP crystals for SHG were operated at the PM temperature (80 °C). If the PMV generated in the first KDP crystal is not compensated for (in which case the structure can be regarded as the traditional method employing a single crystal), the SHG efficiency will rapidly decline, as indicated by the circle symbols in Fig. 2(a). The TAB is 17.8 °C as defined by the full-width at half maximum (FWHM). If the PMV is compensated for and reach an integer multiple of 2π, the TAB becomes 2.1 times larger than that of a single crystal, increasing to 37.1 °C (see the square symbols in Fig. 2(a)).

In the THG experiment, the measured SHG efficiency was 9.6%. The measured maximum THG efficiency was 3.7% when the KDP crystals for THG were operated at the PM temperature. The TAB from the traditional method is 5.2 °C (circle symbols in Fig. 2(b)). If the PMV is compensated for and reach an integer multiple of 2π, the TAB is 12.0 °C, which is 2.3 times larger than that of the traditional method, as shown by the square symbols in Fig. 2(b). Comparing Fig. 2(a) and (b), it can be seen that THG efficiency is more temperature sensitive than SHG efficiency.

According to theoretical calculations, the maximum variation of the PMV of SHG and THG in the KD*P crystal can reach up to 15.33 and 15.82 ($>2\pi$), respectively. The PMV can be well compensated for as long as the maximum variation of the PMV in the electro-optic crystal can reach 2π [18]. Therefore, the period of voltage change for SHG and THG phase mismatch compensation were calculated to be 4.92 and 4.77 kV, respectively. As our high-voltage generator was unstable at low voltage, we chose a voltage range of 5–10 kV in the experiment. The voltages obtained at various temperatures are shown in Fig. 2(c) and (d).

The numerical calculations corresponding to the experimental conditions are shown in Fig. 2(a) and (b) (solid and dashed lines). A comparison between the experimental and calculated results for temperature insensitive SHG and THG is shown in Table 1.

As can be observed from Table 1, the experimental data is in good agreement with the theoretical results, and the proposed method was effective in reducing the temperature sensitivity of the conversion efficiency. However, we note that the experimental TABs are slightly larger than the calculated results for the same case. The reason may be that the actual temperature of the KDP crystals and the display temperature of the ovens were different, especially for a large temperature

TABLE I
Comparison Between Experimental and Calculated Results for Temperature Insensitive SHG and THG

	Parameters	Experimental	Calculated
SHG	TAB without compensation	17.8 °C	15.4 °C
	TAB with compensation	37.1 °C	31.2 °C
	Increase	2.1 times	2.0 times
THG	TAB without compensation	5.2 °C	5.2 °C
	TAB with compensation	12.0 °C	11.1 °C
	Increase	2.3 times	2.1 times

deviation from the PM temperature. The temperature variation range for THG is less than that for SHG; therefore, THG efficiencies are more in line with the theoretical results than SHG efficiencies. Nonetheless, the above results demonstrate that this method can compensate for the PMV effectively and increase the TAB significantly.

3. Discussions

3.1. Analysis at a High Power Density

For high power laser systems, the laser power density can reach up to 2 GW/cm^2 or higher [9], [20]. In the case of high power density, conversion efficiency is very high and is more sensitive to temperature, especially for THG [18]. We considered THG with a FW power density of 2 GW/cm^2 as an example to numerically analyze the frequency conversion. The temporal waveform and transverse spatial profile of the FW are the same as before. The lengths of the KDP crystals for SHG and THG are 12.5 and 11.0 mm, respectively. The PM temperature is set to 20 °C. In order to analyze the temperature-dependent THG efficiency, we assume that the KDP crystal for SHG is always at the PM temperature. The SHG efficiency is 61.2%. The calculated results are shown in Fig. 3.

The TAB of using a traditional single KDP crystal with 11.0 mm length for THG is 3.8 °C (as shown by the solid line in Fig. 3(a)) and the maximum conversion efficiency is 74.6%. If two KDP crystals of equal lengths are cascaded (i.e., 5.5 + 5.5 mm), and the PMV is compensated for and reach an integer multiple of 2π, the TAB increases to 13.0 °C, which is 3.4 times that of a single crystal (as indicated by the dashed line in Fig. 3(a)).

The stability of conversion efficiency is an important parameter of frequency conversion in large laser systems [8]. For THG by a single KDP crystal, the efficiency stable temperature region (ESTR) is only 0.8 °C as defined by the full-width at which the efficiencies fall to 97% of their maximum value. For KDP crystals with a length ratio (LR) of 1:1, ESTR can reach up to 2.95 °C (dashed line in Fig. 3(b)). Based on this method, ESTR can be further improved by optimizing the length of the two KDP crystals. We take two KDP crystals with an LR of 1:2 (i.e., 3.67 + 7.33 mm) as an example to analyze. When the beams emit from the first KDP crystal, the PMV is ΔK_1 ($\Delta K_1 = \Delta k_1 \times L_1$, where Δk_1 and L_1 indicate the phase mismatch and length of the first KDP crystal, respectively). The PMV that should be compensated for is $-2\Delta K_1$ in the electro-optic crystal. Thus, the PMV is $-\Delta K_1$ when the beams incident on the next KDP crystal. The ESTR can reach 4.41 °C, which is 5.5 times larger than that of the traditional method employing a single KDP crystal, as shown by the short-dashed line in Fig. 3(b).

It can be seen from Fig. 3(a) that the generated TH has back-converted completely (i.e., the THG output efficiency is zero) at 24 °C using the traditional method. If the PMV is compensated for by the

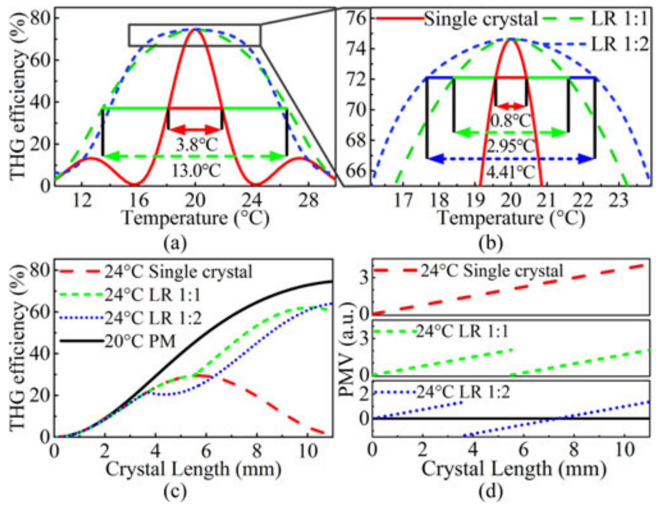

Fig. 3. (a) and (b) Temperature-dependent THG efficiencies. (c) Evolutions of the TH and (d) changes of PMV under combinations of different KDP crystals lengths at 24 °C.

proposed method, the output efficiency can be increased significantly. In order to clearly illustrate the physical process of this method, we take 24 °C as an example and show the evolutions of the TH [see Fig. 3(c)], as well as the changes of the PMV [see Fig. 3(d)] in the KDP crystals under combinations of different crystals lengths.

3.2. Solution of Uneven Temperature

For a high average power laser, the thermal effect of the laser, which is generated by the optical absorption of the nonlinear and electro-optic crystals, will lead to a non-uniform distribution of temperature in the transverse section of the beams. This problem can be solved by optimizing the length of the electro-optic crystal. At the PM temperature T_0 ($\Delta k_1(T_0) = 0$), the beams in the electro-optic crystal need to satisfy

$$\Delta k\,(T_0) \cdot L = N \cdot 2\pi \tag{1}$$

where N is an integer, and L is the length of the electro-optic crystal. This can easily be achieved by adjusting the voltage. Taking into account that absorption has occurred in both the nonlinear and electro-optic crystals, a temperature gradient is present in the transverse section of the beams. When the temperature of the crystals changes, the phase mismatch in the nonlinear and electro-optic crystals can be written as

$$\Delta k_1\,(T) = \Delta k_1\,(T_0) + \Delta k_1' \cdot \Delta T = \Delta k_1' \cdot \Delta T \tag{2}$$

$$\Delta k\,(T) = \Delta k\,(T_0) + \Delta k' \cdot \Delta T \tag{3}$$

where $\Delta k_1' = \partial \Delta k_1(T)/\partial T$, $\Delta k' = \partial \Delta k(T)/\partial T$, $\Delta T = T - T_0$, and T is the crystal temperature. We take two nonlinear crystals of equal lengths as an example to analyze. In order to compensate for the PMV that has accumulated in the first crystal, the following relationship must be satisfied in the electro-optic crystal:

$$\Delta k_1\,(T) \cdot L_1 + \Delta k\,(T) \cdot L = N \cdot 2\pi. \tag{4}$$

Using (1)–(4), the following relationship can be obtained:

$$\Delta k' \cdot L = -\Delta k_1' \cdot L_1. \tag{5}$$

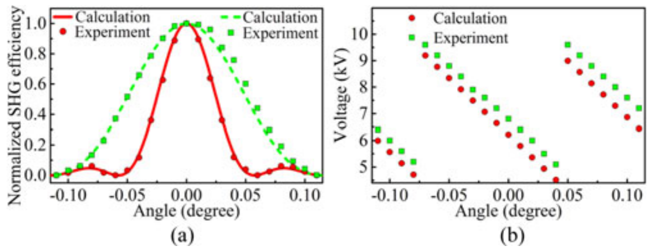

Fig. 4. Experimental and calculated (a) SHG efficiencies and (b) SHG phase mismatch compensation voltages versus angle. In (a), the solid line and circle symbols indicate the traditional method, the dashed line and square symbols indicate our proposed method; and all efficiencies are normalized to their maximum values at the PM angle.

The required electro-optic crystal length is given by

$$L = -\Delta k_1' \cdot L_1 / \Delta k' \tag{6}$$

It can be seen from (6) that $\Delta k_1'$ and $\Delta k'$ need to have opposite signs. This can be achieved by selecting the polarization directions of the beams in the electro-optic crystal. Taking the type-I PM SHG using KDP crystals as an example, the FW and SH are ordinary light and extraordinary light, respectively, in the KDP crystals. When the beams are propagating through the electro-optic crystal, we can configure the FW and SH as extraordinary light and ordinary light, respectively. Thus, $\Delta k_1'$ and $\Delta k'$ have opposite signs, and phase mismatch compensation can be achieved for a non-uniform temperature. For the KDP crystals, which are used for SHG and THG in this paper, the required electro-optic crystal lengths are 3.26 and 2.97 mm, respectively. For the other frequency conversions, the required electro-optic crystal length can be obtained by a similar calculation.

3.3. Angle Insensitive Frequency Conversion

The influence of various unfavorable factors on frequency conversion can be reduced in our proposed method because of its excellent tunability. In order to convincingly verify the versatility of this method, we take the SHG as an example to demonstrate the angle insensitive frequency conversion. In the experiment, two 6.25 mm long KDP crystals for SHG are placed on the optical adjusting brackets with an adjustment precision of 0.01°. The crystals are always at room temperature. The angles of the KDP crystals are varied by 0.01° at a time. The experimental and calculated results are shown in Fig. 4.

The experimentally measured angle acceptance bandwidth (AAB) of SHG from the traditional method is 0.042°, as indicated by the circle symbols in Fig. 4(a). If the PMV is compensated for by the proposed method, the AAB is 0.101° (square symbols in Fig. 4(a)), which is 2.4 times larger than that of traditional method. The corresponding voltages vary with angle as shown in Fig. 4(b).

The results of experiment and analysis shown above indicate that the influence of crystal temperature and angle variation on frequency conversion can be significantly reduced. It is worth noting that this design only needs to satisfy the conditions that laser wavelength falling in the transmission region of the electro-optic crystal and the maximum variation of the PMV over 2π in the electro-optic crystal. The phase mismatch can be well compensated. Therefore, this method is independent of the nonlinear crystal type and the laser wavelength and can be applied to both type-I and type-II PM frequency conversion.

4. Conclusions

In summary, we have designed and experimentally demonstrated a versatile frequency conversion method, which can achieve multi-factors insensitive frequency conversion by applying the electro-optic effect to frequency conversion process. Temperature insensitive SHG and THG and angle insensitive SHG are achieved using a same electro-optic crystal. The experimental results indicated that the TAB and AAB from the proposed method can be two to three times larger than those of the traditional method. The stability of conversion efficiency can be significantly improved. In addition, the optimization of the crystal lengths and the solution for the case of a non-uniform temperature are also given. The phase mismatch arising from various causes can be simultaneously compensated for, since this method has excellent tunability. The influence of various unfavorable factors on frequency conversion can be significantly reduced. More importantly, the method is not limited by the type of nonlinear crystal and is valid for a wide spectral range and can be applied to various frequency conversion processes. The flexibility, versatility and high control precision of this method are incomparable. This method may have potentially important applications in ultraviolet pulse generation and provide a promising approach for designing new-type frequency conversion system.

References

[1] C. Schäfer, C. Fries, C. Theobald, and J. A. L'huillier, "Mode-locking of a high power, 888 nm pumped Nd: YVO 4 laser using nonlinear polarization rotation via Type I second harmonic generation," *Opt. Lett.*, vol. 38, no. 2, pp. 160–162, Jan. 2013.

[2] J. Trull *et al.*, "Ultrashort pulse chirp measurement via transverse second-harmonic generation in strontium barium niobate crystal," *Appl. Phys. Lett.*, vol. 106, no. 22, Jun. 2015, Art. no. 221108.

[3] K. A. Fedorova, G. S. Sokolovskii, P. R. Battle, D. A. Livshits, and E. U. Rafailov, "574–647 nm wavelength tuning by second-harmonic generation from diode-pumped PPKTP waveguides," *Opt. Lett.*, vol. 40, no. 5, pp. 835–838, Mar. 2015.

[4] R. W. Boyd, *Nonlinear Optics*, 3rd ed. New York, NY, USA: Academic, 2008.

[5] R. C. Eckardt and J. Reintjes, "Phase matching limitations of high efficiency second harmonic generation," *IEEE J. Quantum Electron.*, vol. 20, no. 10, pp. 1178–1187, Oct. 1984.

[6] M. Webb, "Temperature sensitivity of KDP for phase-matched frequency conversion of 1 μm laser light," *IEEE J. Quantum Electron.*, vol. 30, no. 8, pp. 1934–1942, Aug. 1994.

[7] N. G. R. Broderick, R. T. Bratfalean, T. M. Monro, D. J. Richardson, and C. M. de Sterke, "Temperature and wavelength tuning of second-, third-, and fourth-harmonic generation in a two-dimensional hexagonally poled nonlinear crystal," *J. Opt. Soc. Amer. B*, vol. 19, no. 9, pp. 2263–2272, Sep. 2002.

[8] M. Shaw, W. Williams, R. House, and C. Haynam, "Laser performance operations model," *Opt. Eng.*, vol. 43, no. 12, pp. 2885–2895, Dec. 2004.

[9] C. A. Haynam *et al.*, "National Ignition Facility laser performance status," *Appl. Opt.*, vol. 46, no. 16, pp. 3276–3303, Jun. 2007.

[10] A. Godard, M. Raybaut, T. Schmid, M. Lefebvre, A. M. Michel, and M. Pealat, "Management of thermal effects in high-repetition-rate pulsed optical parametric oscillators," *Opt. Lett.*, vol. 35, no. 21, pp. 3667–3669, Nov. 2010.

[11] Y. C. Liang, R. F. Su, L. H. Lu, and H. T. Liu, "Temperature nonuniformity occurring during the cooling process of a KDP crystal and its effects on second harmonic generation," *Appl. Opt.*, vol. 53, no. 23, pp. 5109–5116, Aug. 2014.

[12] H. Z. Zhong, P. Yuan, H. Y. Zhu, and L. J. Qian, "Versatile temperature-insensitive second-harmonic generation by compensating thermally induced phase-mismatch in a two-crystal design," *Laser Phys. Lett.*, vol. 9, no. 6, pp. 434–439, Jun. 2012.

[13] L. L. Wang, Y. Chen, and G. C. Liu, "Increased temperature acceptance bandwidth in frequency-doubling process using two different crystals," *Chin. Opt. Lett.*, vol. 12, no. 11, Nov. 2014, Art. no. 111902.

[14] H. Z. Zhong, P. Yuan, S. C. Wen, and L. J. Qian, "Temperature-insensitive frequency tripling for generating high-average power UV lasers," *Opt. Exp.*, vol. 22, no. 4, pp. 4267–4276, Feb. 2014.

[15] J. Chen, Y. Zheng, N. An, and X. Chen, "Noncollinear third-harmonic generation with large angular acceptance by noncritical phase matching in KDP crystal," *Opt. Lett.*, vol. 40, no. 19, pp. 4484–4487, Oct. 2015.

[16] P. Gross *et al.*, "Wide wavelength tuning of an optical parametric oscillator through electro-optic shaping of the gain spectrum," *Opt. Lett.*, vol. 27, no. 16, pp. 1433–1435, Aug. 2002.

[17] H. Ridderbusch *et al.*, "Electro-optic modification of second-harmonic phase-matching spectra in segmented periodically poled $LiNbO_3$," *J. Opt. Soc. Amer. B*, vol. 19, no. 2, pp. 280–288, Feb. 2002.

[18] Z. J. Cui, D. A. Liu, M. Z. Sun, J. Miao, and J. Q. Zhu, "Compensation method for temperature-induced phase mismatch during frequency conversion in high-power laser systems," *J. Opt. Soc. Amer. B*, vol. 33, no. 4, pp. 525–534, Apr. 2016.

[19] D. N. Nikogosyan, *Nonlinear Optical Crystals: A Complete Survey*. New York, NY, USA: Springer, 2005.

[20] L. L. Ji, B. Q. Zhu, C. Liu, T. Wang, and Z. Q. Lin, "Optimization of quadrature frequency conversion with type-II KDP for second harmonic generation of the nanosecond chirp pulse at 1053 nm," *Chin. Opt. Lett.*, vol. 12, no. 3, Mar. 2014, Art. no. 031902.